Scaled opposite-spin CC2 for ground and excited states with fourth order scaling computational costs

Nina O. C. Winter[a] and Christof Hättig[b]
Lehrstuhl für Theoretische Chemie, Ruhr-Universität Bochum, 44801 Bochum, Germany

(Received 25 February 2011; accepted 11 April 2011; published online 9 May 2011)

An implementation of scaled opposite-spin CC2 (SOS-CC2) for ground and excited state energies is presented that requires only fourth order scaling computational costs. The SOS-CC2 method yields results with an accuracy comparable to the unscaled method. Furthermore the time-determining fifth order scaling steps in the algorithm can be replaced by only fourth order scaling computational costs using a "resolution of the identity" approximation for the electron repulsion integrals and a Laplace transformation of the orbital energy denominators. This leads to a significant reduction of computational costs especially for large systems. Timings for ground and excited state calculations are shown and the error of the Laplace transformation is investigated. An application to a chlorophyll molecule with 134 atoms results in a speed-up by a factor of five and demonstrates how the new implementation extends the applicability of the method. A SOS variant of the algebraic diagrammatic construction through second order ADC(2), which arises from a simplification of the SOS-CC2 model, is also presented. The SOS-ADC(2) model is a cost-efficient alternative in particular for future extensions to spectral intensities and excited state structure optimizations. © *2011 American Institute of Physics*. [doi:10.1063/1.3584177]

I. INTRODUCTION

Density functional theory (DFT) is a widely used tool in quantum chemistry since it is robust and requires low computational costs. The calculation of excited states of large molecules is possible by using the time-dependent variant of DFT, TDDFT. However, today's semilocal functionals provide a poor description of dispersion interactions and weak intermolecular bonds and fail at the description of charge transfer states.

In 2003 the idea of spin scaling was introduced by Stefan Grimme.[1] He proposed an empirical scaling of the same and opposite spin contributions (spin component scaling, SCS) to the MP2 energy. By the introduction of empirical scaling factors, the deviation of the MP2 results from accurate reference data was reduced without increasing computational costs. As the scaling factor for the same spin part in the SCS approach was much smaller than the scaling factor for the opposite spin part, the idea came up to neglect the same spin part completely. Jung *et al.* noticed that this scaled opposite spin (SOS) ansatz can be implemented with only fourth order scaling computational costs.[2] The idea of spin scaling was also applied to the description of excited states. Grimme *et al.* proposed a SCS variant of CIS(D).[3] Rhee *et al.* presented a fourth order scaling implementation of excited state energies for SOS-CIS(D) (Ref. 4) and gradients for excited states in the framework of SOS-CIS(D_0).[5]

With the fourth order scaling SOS-CIS(D) model there is a computational tool available that can describe excited states with an accuracy comparable to unscaled CIS(D) and requires significantly lower costs. However, the perturbative correction in CIS(D) theory requires that the excited state wavefunction is already described accurately by configuration interaction singles (CIS). The non-degenerate perturbation theory used in CIS(D) cannot deal with avoided crossings. This leads to serious problems, especially for geometry optimizations in the excited state, if there are other states of the same symmetry close by.

In CIS(D_0) this problem is avoided by applying degenerate perturbation theory. This is done at the expense of neglecting the excitation frequency in the orbital denominators, which is unphysical. Another disadvantage of the CIS(D) based approximations is that they do not provide a straightforward route for transition properties as one- and two-photon transition strengths and frequency-dependent properties.

CC2[6] is a coupled cluster method, for which excited state energies, gradients, transition moments, and frequency dependent properties can be derived in a straightforward manner using the framework of coupled cluster response theory.[7–10] The computational costs of conventional CC2 increase as for MP2 and CIS(D) with fifth order of the system size. One route to reduce the scaling of these methods are local correlation approaches.[11] The computational savings of local approaches for excited states are, however, not as large as for the ground state. The SOS approximation is an alternative, although partially empirical, route to reduce the computational complexity of second-order methods like MP2 or CC2. It was shown that SOS-CC2 provides an accuracy comparable to unscaled CC2.[12] At the same time SOS-CC2 can be implemented with only fourth order scaling computational costs, similar to SOS-MP2 and SOS-CIS(D).

We report here a fourth order scaling implementation of SOS-CC2 for ground and electronically excited state energies in the TURBOMOLE program package.[13]

[a]Electronic mail: Nina.Winter@theochem.rub.de.
[b]Electronic mail: Christof.Haettig@rub.de.

 © 2011 American Institute of Physics

Downloaded 09 May 2011 to 134.147.252.238. Redistribution subject to AIP license or copyright; see http://jcp.aip.org/about/rights_and_permissions

II. THEORY

A. Scaled opposite spin CC2

The SOS-CC2 energy is given by:[12]

$$E_{\mathrm{CC2}}^{\mathrm{SOS}} = \langle \mathrm{HF}|\tilde{\hat{H}} + \mathrm{c_{os}}[\tilde{\hat{H}}, \hat{\mathrm{T}}_2^{\mathrm{os}}]|\mathrm{HF}\rangle, \tag{1}$$

where $\tilde{\hat{H}}$ is the similarity-transformed Hamiltonian $\tilde{\hat{H}} = e^{-\hat{T}_1}\hat{H}e^{\hat{T}_1}$ and $\hat{T}_2^{\mathrm{OS}}$ is the two electron excitation operator, which acts on two electrons with different spins.

The wavefunction parameters for SOS-CC2 are determined by the CC2 cluster equations for singles and doubles

$$\Omega_{\mu_1} = \langle \mu_1|\tilde{\hat{H}} + c_{\mathrm{os}}[\tilde{\hat{H}}, \hat{T}_2^{\mathrm{os}}]|\mathrm{HF}\rangle = 0, \tag{2}$$

$$\Omega_{\mu_2} = \langle \mu_2^{\mathrm{os}}|\tilde{\hat{H}} + [\hat{F}, \hat{T}_2^{\mathrm{os}}]|\mathrm{HF}\rangle = 0, \tag{3}$$

where μ_1 are singly excited determinants and μ_2^{os} are doubly excited determinants generated from the excitations included in $\hat{T}_2^{\mathrm{os}}$. The SOS-CC2 model is designed such that it leads directly to SOS-MP2 if one neglects the singles contribution. The scaling in the equation for the singles is applied to the term, which is second order in perturbation theory $[\tilde{\hat{H}}, \hat{T}_2^{\mathrm{os}}]$. We use the same scaling factor as for SOS-MP2, namely, $c_{\mathrm{os}} = 1.3$.

B. Excited states

In the framework of coupled cluster methods excited states are described within response theory. Vertical excitation energies are obtained as eigenvalues of the SOS-CC2 Jacobi matrix:

$$\mathbf{A} = \begin{pmatrix} \mathbf{A}_{\mu_1\nu_1} & \mathbf{A}_{\mu_1\nu_2} \\ \mathbf{A}_{\mu_2\nu_2} & \mathbf{A}_{\mu_2\nu_2} \end{pmatrix} = \begin{pmatrix} \langle \mu_1|[(\tilde{\hat{H}} + c_{\mathrm{os}}[\tilde{\hat{H}}, \hat{T}_2^{\mathrm{os}}]), \hat{\tau}_{\nu_1}]|\mathrm{HF}\rangle & \langle \mu_1|c_{\mathrm{os}}[\tilde{\hat{H}}, \hat{\tau}_{\nu_2}^{\mathrm{os}}]|\mathrm{HF}\rangle \\ \langle \mu_2^{\mathrm{os}}|[\tilde{\hat{H}}, \hat{\tau}_{\nu_1}]|\mathrm{HF}\rangle & \langle \mu_2^{\mathrm{os}}|[\hat{F}, \hat{\tau}_2^{\mathrm{os}}]|\mathrm{HF}\rangle \end{pmatrix}. \tag{4}$$

An important property of the CC2 method is that with canonical orbitals the doubles/doubles block of the Jacobi matrix $\mathbf{A}_{\mu_2\nu_2}$ is diagonal, where the diagonal elements are the orbital energy differences $\epsilon_a - \epsilon_i + \epsilon_b - \epsilon_j = \epsilon_{aibj}$. Thereby we can express the CC2 eigenvalue problem as an effective eigenvalue problem in the space of the single excitations:

$$\left[\mathbf{A}_{\mu_1\nu_1} - \sum_{\mu_2} \frac{\mathbf{A}_{\mu_1\mu_2}\mathbf{A}_{\mu_2\nu_1}}{\epsilon_{\mu_2} - \omega}\right]\mathbf{E}_{\nu_1} = \omega\mathbf{E}_{\mu_1}. \tag{5}$$

One can partition the singles/singles block of the effective CC2 Jacobian into a part $\mathbf{A}_{\mu_1\nu_1}^{(0)}$ independent of $\hat{T}_2$ and $\mathbf{A}_{\mu_1\nu_1}^{(2)}(\hat{T}_2)$. If we express the effective eigenvalue problem in terms of the non-scaled matrices $\mathbf{A}^{\mathrm{ns}}$, the spin scaling can be applied as following:

$$\left[\mathbf{A}_{\mu_1\nu_1}^{(0),\mathrm{ns}} + c_{\mathrm{os}}^{\mathrm{gs}}\mathbf{A}_{\mu_1\nu_1}^{(2),\mathrm{ns}}(\hat{T}_2^{\mathrm{os}}) - c_{\mathrm{os}}^{\mathrm{ex}}\sum_{\mu_2} \frac{\mathbf{A}_{\mu_1\mu_2}^{\mathrm{ns,os}}\mathbf{A}_{\mu_2\nu_1}^{\mathrm{ns,os}}}{\epsilon_{\mu_2} - c_\omega\omega}\right]\mathbf{E}_{\nu_1} = \omega\mathbf{E}_{\mu_1}. \tag{6}$$

In this equation the term $\mathbf{A}_{\mu_1\nu_1}^{(2),\mathrm{ns}}(\hat{T}_2^{\mathrm{os}})$ accounts for the correlation effects coming from the ground state and the last term on the left hand side describes dynamic electron correlation effects in the excited state. Two different scaling factors $c_{\mathrm{os}}^{\mathrm{gs}}$ and $c_{\mathrm{os}}^{\mathrm{ex}}$ for the ground and excited state correlation contributions and a damping factor for the excitation frequency in the denominator c_ω can be applied for this parameterization. Thereby we get the SOS-CIS(D) model proposed by Rhee and Head-Gordon[4] from our SOS-CC2 model in the same way as unscaled CIS(D) can be derived from unscaled CC2. For our study we used the same scaling factor for ground and excited state contributions $c_{\mathrm{os}}^{\mathrm{gs}} = c_{\mathrm{os}}^{\mathrm{ex}} = 1.3$ and employed $c_\omega = 1$.

C. Simplified approaches: SOS-CIS(D_∞) and SOS-ADC(2)

The CIS(D_∞) approach introduced by Head-Gordon *et al.*[14] can be derived from CC2 theory by setting the singles part of the ground state cluster amplitudes $\hat{T}_1$ equal to zero. This means that the similarity transformation of the Hamiltonian vanishes so that the Jacobi matrix is calculated from the non-transformed Hamiltonian:

$$\mathbf{A}^{\mathrm{CIS(D}_\infty)} = \begin{pmatrix} \langle \mu_1|[(\hat{H} + c_{\mathrm{os}}[\hat{H}, \hat{T}_2^{(1),\mathrm{os}}]), \hat{\tau}_{\nu_1}]|\mathrm{HF}\rangle & \langle \mu_1|c_{\mathrm{os}}[\hat{H}, \hat{\tau}_{\nu_2}^{\mathrm{os}}]|\mathrm{HF}\rangle \\ \langle \mu_2^{\mathrm{os}}|[\hat{H}, \hat{\tau}_{\nu_1}]|\mathrm{HF}\rangle & \langle \mu_2^{\mathrm{os}}|[\hat{F}, \hat{\tau}_2^{\mathrm{os}}]|\mathrm{HF}\rangle \end{pmatrix}. \tag{7}$$

Downloaded 09 May 2011 to 134.147.252.238. Redistribution subject to AIP license or copyright; see http://jcp.aip.org/about/rights_and_permissions

The secular matrix for the algebraic diagrammatic construction through second order ADC(2) (Ref. 15) is related to the CIS(D_∞) Jacobi matrix by a symmetrization:

$$\mathbf{A}^{\mathrm{ADC(2)}} = \frac{1}{2}(\mathbf{A}^{\mathrm{CIS(D_\infty)}} + (\mathbf{A}^{\mathrm{CIS(D_\infty)}})^\dagger). \tag{8}$$

The SOS versions of CIS(D_∞) and ADC(2) are related to SOS-CC2 in the same way as unscaled CIS(D_∞) and ADC(2) to unscaled CC2. A fourth-order scaling implementation of these models is thus obtained as a byproduct of the SOS-CC2 implementation.

III. IMPLEMENTATION

A. Prerequisites

To get a fourth order scaling algorithm for the CC2 energy, the four-index electron repulsion integrals (ERIs) are decomposed by a resolution-of-the-identity (RI) approximation:

$$(pq|rs) = \sum_P B^P_{pq}\, B^P_{rs} \tag{9}$$

with the three-index intermediates

$$B^P_{pq} = \sum_{\alpha\beta Q} C_{\alpha p} C_{\beta q}\, (\alpha\beta|Q)\, [V^{-1/2}]_{QP} \tag{10}$$

to bypass an expensive four-index AO to MO transformation. In the latter equations p, q, r, s are MO indices, α, β are AO indices and P, Q are auxiliary functions for the RI approximation. $(\alpha\beta|Q)$ are three-index and $V_{QP} = (Q|P)$ two-index ERIs. $\mathbf{C}$ is the MO coefficient matrix.

In the CC2 model expressions occur, which are most conveniently formulated in terms of the integrals for the similarity-transformed Hamiltonian $\tilde{\hat{H}}$. The electron repulsion integrals $(p\hat{q}|rs) = \sum_P \hat{B}^P_{pq}\, \hat{B}^P_{rs}$ are modified with the singles part of the cluster amplitudes $\mathbf{t}_1$. They can be formed from the three-index intermediates

$$\hat{B}^P_{pq} = \sum_{\alpha\beta Q} \Lambda^p_{\alpha p} \Lambda^h_{\beta q}\, (\alpha\beta|Q)\, [V^{-1/2}]_{QP} \tag{11}$$

with the transformation matrices given by

$$\Lambda^p = \mathbf{C}(\mathbf{1} - \mathbf{t}_1^T), \tag{12}$$

$$\Lambda^h = \mathbf{C}(\mathbf{1} + \mathbf{t}_1). \tag{13}$$

The modified Fock matrix is built from the integrals of $\tilde{\hat{H}}$

$$\hat{F}_{pq} = \hat{h}_{pq} + \sum_{rs}(2(rs|pq) - (rq|ps)), \tag{14}$$

where the modified one-electron integrals $\hat{h}_{pq}$ are related to the conventional AO integrals $h_{\alpha\beta}$ in the same way as $(p\hat{q}|rs)$ is related to $(\alpha\beta|\gamma\delta)$, i.e., $\hat{h}_{pq} = \sum_{\alpha\beta} \Lambda^p_{\alpha p} \Lambda^h_{\beta q} h_{\alpha\beta}$.

To describe excited states within CC2 theory, expressions are needed that depend on the singles part of the right eigenvector. To solve the eigenvalue problem in Eq. (6) additional integrals are used, which depend on the singles part of the right eigenvector or a trial vector $\mathbf{R}_1$. We define the electron repulsion integrals $(p\bar{q}|rs) = \sum_P \bar{B}^P_{pq} \hat{B}^P_{rs} + \hat{B}^P_{pq} \bar{B}^P_{rs}$ with the three-index quantities

$$\bar{B}^P_{pq} = \sum_{\alpha\beta Q} \left(\bar{\Lambda}^p_{\alpha p} \Lambda^h_{\beta q} + \Lambda^p_{\alpha p} \bar{\Lambda}^h_{\beta q}\right)(\alpha\beta|Q)\, [V^{-1/2}]_{QP} \tag{15}$$

calculated from the transformation matrices $\bar{\Lambda}^p = -\mathbf{C}\mathbf{R}_1^T$ and $\bar{\Lambda}^h = \mathbf{C}\mathbf{R}_1$.

B. Cluster equations

The singles part of the ground state vector function Ω_{ai} from Eq. (2) can be partitioned as follows:

$$\Omega_{ai} = \Omega^G_{ai} + \Omega^H_{ai} + \Omega^I_{ai} + \Omega^J_{ai}. \tag{16}$$

The working expressions for the individual terms of the vector function can be formulated in terms of computational convenient intermediates as shown in Table I. The time-determining steps are the calculation of Ω^I_{ai} and of the intermediate

$$Y^Q_{ai} = c_{os} \sum_{bj} t^{ab}_{ij}\, B^Q_{bj}. \tag{17}$$

Within the RI approximation the SOS-CC2 cluster amplitudes are given by

$$t^{ab}_{ij} = -\frac{\sum_P \hat{B}^P_{ai} \hat{B}^P_{bj}}{\epsilon_a - \epsilon_i + \epsilon_b - \epsilon_j}, \tag{18}$$

where $\hat{B}^P_{ai}$ is defined in Eq. (11). To get the fourth order scaling algorithm, we use a Laplace transformation followed by a numerical quadrature to factorize the orbital energy denominator $\frac{1}{\epsilon_{aibj}}$ with $\epsilon_{aibj} = \epsilon_a - \epsilon_i + \epsilon_b - \epsilon_j$ as:

$$\frac{1}{\epsilon_{aibj}} = \int_0^\infty e^{-\epsilon_{aibj} t} dt \approx \sum_z^n w_z\, e^{-\epsilon_{aibj} t_z}$$

$$= \sum_z^n w_z (e^{-\epsilon_{ai} t_z} \cdot e^{-\epsilon_{bj} t_z}), \tag{19}$$

where $\epsilon_{ai} = \epsilon_a - \epsilon_i$ and $\epsilon_{bj} = \epsilon_b - \epsilon_j$. The w_z are the weights and the t_z the grid points of the numerical quadrature

TABLE I. Explicit expressions for the SOS-CC2 vector function and for a trial vector linear transformed with the effective Jacobian. The single excitation part of the vector function is written as $\Omega_{ai} = \Omega^G_{ai} + \Omega^H_{ai} + \Omega^I_{ai} + \Omega^J_{ai}$. The transformed vector is given by $\sigma_{ai}(\omega, R_1) = \sigma^0_{ai} + \sigma^G_{ai} + \sigma^H_{ai} + \sigma^I_{ai} + \sigma^J_{ai}$.

	$\sigma^0_{ai} = \sum_b E^{(1)}_{ab} R_{bi} - \sum_j R_{aj} E^{(2)}_{ji}$
$\Omega^G_{ai} = +\sum_{c,Q} Y^Q_{ci}\, B^Q_{ac}$	$\sigma^G_{ai} = +\sum_{c,Q} \bar{Y}^Q_{ci}\, B^Q_{ac}$
$\Omega^H_{ai} = -\sum_{k,Q} Y^Q_{ak}\, B^Q_{ki}$	$\sigma^H_{ai} = -\sum_{k,Q} \bar{Y}^Q_{ak}\, B^Q_{ki}$
$\Omega^I_{ai} = \sum_{dl} t^{ad}_{il}\, \hat{F}_{ld}$	$\sigma^I_{ai} = \sum_{dl} (R^{ad}_{il}\, \hat{F}_{ld} + t^{ad}_{il}\, \bar{F}_{ld})$
$\Omega^J_{ai} = \hat{F}_{ai}$	$\sigma^J_{ai} = \bar{F}'_{ai}$
$Y^Q_{ai} = \sum_{bj} t^{ab}_{ij}\, B^Q_{bj}$	$E^{(1)}_{ab} = \hat{F}_{ab} - \sum_{k,Q} Y^Q_{ak}\, B^Q_{kb}$
$\bar{Y}^Q_{ai} = \sum_{bj} R^{ab}_{ij}\, B^Q_{bj}$	$E^{(2)}_{ij} = \hat{F}_{ij} + \sum_{c,Q} Y^Q_{ci}\, B^Q_{jc}$
	$\bar{F}_{ld} = \sum_{ck} (ld\hat{|}kc) R_{ck}$
	$\bar{F}'_{ai} = \sum_{ck} (ai\hat{|}kc) R_{ck}$

Downloaded 09 May 2011 to 134.147.252.238. Redistribution subject to AIP license or copyright; see http://jcp.aip.org/about/rights_and_permissions

procedure. With this approximation the cluster amplitudes can be expressed as

$$t_{ij}^{ab} = -\sum_{z}^{n} w_z \sum_{P} \hat{B}_{ai}^{P}\, e^{-\epsilon_{ai}\, t_z} \cdot \hat{B}_{bj}^{P}\, e^{-\epsilon_{bj}\, t_z}. \tag{20}$$

If we plug the Laplace transformed expression for the cluster amplitudes into Eq. (17) we can evaluate Y_{ai}^{Q} as:

$$Y_{ai}^{Q} = -c_{os} \sum_{z}^{n} w_z \sum_{P} N_z^{QP}\, \hat{B}_{ai}^{P} \cdot e^{-\epsilon_{ai}\, t_z} \tag{21}$$

with

$$N_z^{QP} = \sum_{bj} B_{bj}^{Q}\, \hat{B}_{bj}^{P}\, e^{-\epsilon_{bj}\, t_z}. \tag{22}$$

These two steps can be carried out with only fourth order scaling computational costs. If we plug the Laplace transformed expression for the cluster amplitudes into the equation for Ω_{ai}^{I} we get

$$\Omega_{ai}^{I} = -c_{os} \sum_{z}^{n} w_z \sum_{Q} n_z^{Q}\, \hat{B}_{ai}^{Q}\, e^{-\epsilon_{ai}\, t_z} \tag{23}$$

with

$$n_z^{Q} = \sum_{bj} \hat{F}_{bj}\, \hat{B}_{bj}^{Q}\, e^{-\epsilon_{bj}\, t_z}. \tag{24}$$

These two steps can be carried out with only third order scaling computational costs. All remaining steps for the computation of Ω_{ai} are carried out as for unscaled RI-CC2 with fourth and third order scaling costs.

C. Excited states

The effective eigenvalue problem in Eq. (5) is solved iteratively, which requires the implementation of the linear transformation of a trial vector with the effective Jacobian. The singles part of the linear transformed trial vector can be written as:

$$\sigma_{ai}(\omega, R_1) = \sigma_{ai}^{0} + \sigma_{ai}^{G} + \sigma_{ai}^{H} + \sigma_{ai}^{I} + \sigma_{ai}^{J}. \tag{25}$$

Explicit expressions for the individual contributions to σ_{ai} are given in Table I. The time-determining steps are—similar as for the ground state—the computation of σ_{ai}^{I} and

$$\bar{Y}_{ai}^{Q} = c_{os} \sum_{bj} R_{ij}^{ab}\, B_{bj}^{Q}. \tag{26}$$

The doubles part of the trial vector is given as

$$R_{ij}^{ab} = -\frac{\sum_P \bar{B}_{ai}^{P} \hat{B}_{bj}^{P} + \hat{B}_{ai}^{P} \bar{B}_{bj}^{P}}{\epsilon_a - \epsilon_i + \epsilon_b - \epsilon_j - \omega}, \tag{27}$$

where $\bar{B}_{ai}^{P}$ is defined in Eq. (11). The algorithm for the computation of σ_{ai}^{I} and $\bar{Y}_{ai}^{Q}$ is sketched in Fig. 1. The algorithm can be parallelized easily by assigning a batch of occupied orbitals to each slave node. Each slave node builds the contributions for N_z^{PQ} and n_z^{Q} from the assigned orbitals. After the loop over J the intermediates are summed up on the master node and distributed to the slaves nodes. Each slave node can then calculate the contribution to $\bar{Y}_{ai}^{P}$ and σ_{ai}^{I} for the orbitals assigned to it.

loop over z

  loop over J

    read B_{bj}^{P}, $\hat{B}_{bj}^{Q}$, $\bar{B}_{bj}^{Q}$ for $j \in J$

    $\hat{K}_{bj,z}^{Q} \leftarrow \hat{B}_{bj}^{Q} \cdot e^{-t_z\,(\epsilon_b - \epsilon_j - \omega)}$
    $N_z^{PQ} \leftarrow \sum_{bj} \hat{K}_{bj,z}^{Q}\, B_{bj}^{P}$
    $n_z^{Q} \leftarrow \sum_{bj} \hat{K}_{bj,z}^{Q}\, \hat{F}_{bj}$
    $\bar{n}_z^{Q} \leftarrow \sum_{bj} \hat{K}_{bj,z}^{Q}\, \bar{F}_{bj}$

    $\bar{K}_{bj,z}^{Q} \leftarrow \bar{B}_{bj}^{Q} \cdot e^{-t_z\,(\epsilon_b - \epsilon_j - \omega)}$
    $\bar{N}_z^{PQ} \leftarrow \sum_{bj} \bar{K}_{bj,z}^{Q}\, B_{bj}^{P}$
    $\bar{n}_z^{Q} \leftarrow + \sum_{bj} \bar{K}_{bj,z}^{Q}\, \hat{F}_{bj}$

  end loop over J

  scale N_z^{PQ}, $\bar{N}_z^{PQ}$, n_z^{Q}, $\bar{n}_z^{Q}$ with $-c_{os} w_z$

  loop over I

    read $\bar{Y}_{ai}^{P}$ for $i \in I$

    read $\hat{B}_{bj}^{Q}$, $\bar{B}_{bj}^{Q}$ for $j \in J$

    $\bar{K}_{ai,z}^{Q} \leftarrow \bar{B}_{ai}^{Q} \cdot e^{-t_z\,(\epsilon_a - \epsilon_i - \omega)}$
    $\bar{Y}_{ai}^{P} \leftarrow \sum_{Q,z} N_z^{PQ}\, \bar{K}_{ai,z}^{Q}$
    $\sigma_{ai}^{I} \leftarrow \sum_{Q,z} n_z^{Q}\, \bar{K}_{ai,z}^{Q}$

    $\hat{K}_{ai,z}^{Q} \leftarrow \hat{B}_{ai}^{Q} \cdot e^{-t_z\,(\epsilon_a - \epsilon_i - \omega)}$
    $\bar{Y}_{ai}^{P} \leftarrow + \sum_{Q,z} \bar{N}_z^{PQ}\, \hat{K}_{ai,z}^{Q}$
    $\sigma_{ai}^{I} \leftarrow + \sum_{Q,z} \bar{n}_z^{Q}\, \hat{K}_{ai,z}^{Q}$

    store $\bar{Y}_{ai}^{P}$ on file

  end loop over I

end loop over z

FIG. 1. Algorithm for the calculation of a trial vector linear transformed with the SOS-CC2 Jacobi matrix.

The calculation of σ_{ai}^{0} requires additionally the intermediates $E_{ab}^{(1)}$ and $E_{ij}^{(2)}$. Since these are independent of the trial vector $\mathbf{R}_1$, they can be evaluated once as global intermediates after the solution of the ground state equations.

Downloaded 09 May 2011 to 134.147.252.238. Redistribution subject to AIP license or copyright; see http://jcp.aip.org/about/rights_and_permissions

IV. RESULTS

A. Laplace error

To get a fourth order scaling algorithm the energy denominator $\epsilon_{aibj} = \epsilon_a - \epsilon_i + \epsilon_b - \epsilon_j$ is factorized using a numerical Laplace transformation (see. Eq. (19)). To determine the optimal grid points t_z for the numerical quadrature procedure the error function

$$F^{\mathrm{Lap}}(t_z) = \int_{\epsilon_{\min}}^{\epsilon_{\max}} \left(\frac{1}{\epsilon_{aibj}} - \sum_z^n w_z \, e^{-\epsilon_{aibj} t_z} \right)^2 \qquad (28)$$

is minimized for a fixed number of grid points n on the interval $[\epsilon_{\max}, \epsilon_{\min}]$. For given grid points t_z the weights w_z can be calculated by solving a system of linear equations.[16]

The optimization of the grid points is sensitive to the employed starting guess especially when a small value of the error function F^{Lap} is required.[17] Therefore we first minimize the error function F^{Lap} for a small number of grid points and then increase the number of points successively until the desired accuracy of the numerical quadrature approximation is achieved. Thereby the grid points of the previous minimization processes serve as starting guesses for the following ones. With this strategy the minimization converges reliably and fast to quadrature grids which improve systematically with increasing number of grid points.

The additional error introduced by the numerical quadrature, denoted in the following as Laplace error ΔE^{Lap}, is defined as

$$\Delta E^{\mathrm{Lap}} = E_{\mathrm{SOS}} - E^{\mathrm{Lap}}_{\mathrm{SOS}}, \qquad (29)$$

where $E^{\mathrm{Lap}}_{\mathrm{SOS}}$ is the SOS energy calculated using the fourth order scaling Laplace-transformed algorithm and E_{SOS} is the SOS energy calculated with the conventional fifth order scaling algorithm using only the RI approximation. We first tested the error of the SOS-CC2 ground state energy for a chain of three glycines and a benzene molecule using the SVP,[18] TZVP,[19] TZVPP,[20] and QZVPP (Ref. 21) basis and corresponding auxiliary basis sets for the RI-approximation.[20,22] Further calculations included the inorganic molecules MnO_4^-, $SiCl_4$, and Zn_2 using the TZVP, aug-cc-pVTZ,[23–29] and aug-cc-pwCVTZ (Refs. 22, 25–27, 29, 30) basis sets. The results are shown in Figs. 2 and 3. In nearly all cases the absolute Laplace error is lower than the square root of the error function

$$|\Delta E^{\mathrm{Lap}}| \leq \sqrt{F^{\mathrm{Lap}}}. \qquad (30)$$

The error function F^{Lap} provides thus a reliable upper bound for the Laplace error of the ground state energy.

For excited state calculations the energy denominators also contain the excitations frequency $\epsilon_{aibj} = \epsilon_a - \epsilon_i + \epsilon_b - \epsilon_j - \omega$ (see. Eq. (27)). Thereby the minimal energy denominator $\epsilon_{\min}$ occurring in Eq. (28) is shifted by ω:

$$\epsilon_{\min} = 2(\epsilon_{\mathrm{LUMO}} - \epsilon_{\mathrm{HOMO}}) - \omega. \qquad (31)$$

As the excitation energy ω is not known before the calculation, the optimal interval for the determination of the Laplace grid points is difficult to determine. We tested if the frequency ω can be neglected for the determination of the interval $[\epsilon_{\max}, \epsilon_{\min}]$.

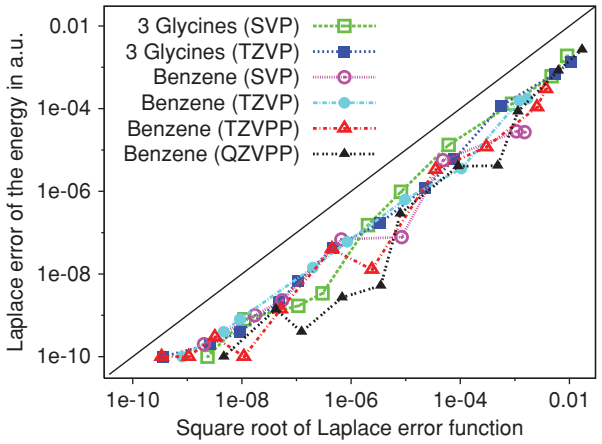


FIG. 2. Absolute Laplace error of the SOS energy $|\Delta E^{\mathrm{Lap}}|$ in a.u. versus the square root of the Laplace error function $\sqrt{F^{\mathrm{Lap}}}$ for a chain of three glycines and the benzene molecule using the SVP, TZVP, TZVPP, and QZVPP basis sets.

For this we evaluated the Laplace error for vertical excitation energies on a set of 89 singlet and 71 triplet excited states. For details of the test set see Sec. IV C. Calculations with different convergence criteria for the Laplace error function F^{Lap} were carried out and compared to SOS-CC2 calculations using the conventional algorithm without Laplace transformation. The results can be seen in Table II. Using a convergence criterion of $\sqrt{F^{\mathrm{Lap}}} < 10^{-4}$, one would expect a Laplace error of less than 0.1 mH or 2.7 meV in the energy. With a Laplace error of 7.84 meV the $2\ ^1B_{3g}$ state of s-tetrazine is the only one, where this is not the case. For all other states the Laplace error is significantly lower than expected from F^{Lap}. This can be seen from the low standard deviation of 0.13 meV. If we have a look at the other convergence criteria, we get the same picture. The Laplace error is higher than expected only for the $2\ ^1B_{3g}$ state of s-tetrazine (see MAX for the values). From a convergence criterion of $\sqrt{F^{\mathrm{Lap}}} < 10^{-3}$ we would expect a Laplace error of the energy of less than 1 mH or 27 meV. The

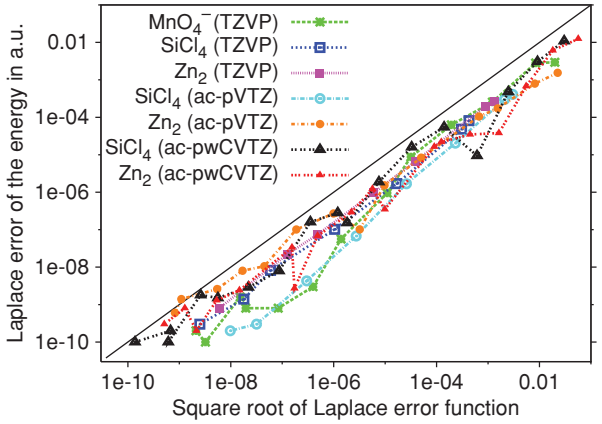


FIG. 3. Absolute Laplace error of the SOS energy $|\Delta E^{\mathrm{Lap}}|$ in a.u. versus the square root of the Laplace error function $\sqrt{F^{\mathrm{Lap}}}$ for MnO_4^-, $SiCl_4$, and Zn_2 using the TZVP, aug-cc-pVTZ (ac-pVTZ), and aug-cc-pwCVTZ (ac-pwCVTZ) basis sets.

Downloaded 09 May 2011 to 134.147.252.238. Redistribution subject to AIP license or copyright; see http://jcp.aip.org/about/rights_and_permissions

TABLE II. Laplace error for excitation energies evaluated for the test set from Tables V and VI. Maximum absolute error (MAX), mean error (ME), mean absolute error (MAE), and standard deviation (SD) in meV are given for different values of the Laplace error function F^{Lap}.

F^{Lap}	10^{-8}	10^{-7}	10^{-6}	10^{-5}	10^{-4}
MAX	7.84	19.91	19.92	32.95	71.83
ME	0.13	0.33	0.47	0.91	1.40
MAE	0.13	0.35	0.51	0.98	2.03
SD	0.64	1.63	1.71	2.81	6.19

standard deviation of 1.71 meV shows that the error is much lower for most of the states. With the aug-cc-pVTZ basis set the error due to the RI approximation is already of the order of meV,[9], so that a Laplace error lower than that is not required. Enforcing $\sqrt{F^{\text{Lap}}} < 10^{-4}$ seven Laplace grid points are used for all molecules of the test set. $\sqrt{F^{\text{Lap}}} < 10^{-3}$ results in five to six grid points. Thus for common applications, six to seven Laplace grid points are sufficient to get a satisfactory accuracy for excitation energies. This number was also found for SOS-CIS(D).[4]

B. Timings

The time-determining steps of the Laplace-transformed SOS-CC2 algorithm scale with $N_x^2 N_o N_v N_L$ (see Eqs. (21) and (22)), where N_x is the number of auxiliary functions for the RI-approximation, N_o is the number of occupied orbitals, N_v the number of virtual orbitals, and N_L the number of grid points for the numerical quadrature, which is independent of the system size. The prefactor of the fourth order scaling steps is two for ground state calculations, as one N intermediate and one Y intermediate (see Eqs. (21) and (22)) have to be calculated. For excited state calculations two N and Y intermediates are needed, which results in a prefactor of four. For conventional CC2 calculations the time-determining steps scale with $N_x N_o^2 N_v^2$. For the ground state the prefactor is $\frac{3}{2}$, as one Y intermediate and the cluster amplitudes (see Eqs. (17) and (18)) have to be built, where for the cluster amplitudes the symmetry $t_{ab}^{ij} = t_{ba}^{ji}$ can be exploited so that they only have to be computed for $i \geq j$. For excited state calculations $\bar{Y}_{ai}^{Q}$ and the doubles part of the right eigenvector (see Eqs. (26) and (27)) are needed. Additionally the ground state cluster amplitudes are formed to calculate σ_{ai}^{I}, which results in a prefactor of $\frac{5}{2}$. If we exploit that $N_x \approx 3N_v$ for most basis sets, the ratio between the operation counts for the fifth and fourth order scaling algorithms is proportional to $\frac{N_o}{N_L}$ with prefactors of $\frac{1}{4}$ for ground state calculations and $\frac{5}{32}$ for excited states. For a fixed number of Laplace grid points the reduction of computational costs with the Laplace-transformed algorithm thus increases with the number of occupied orbitals, which corresponds to the size of the considered molecules.

The savings in computational time with increasing number of atoms is shown for a series of glycine polypeptides. The chain length is varied between two and nine glycines. For these test systems CC2 calculations for ground and excited state energies were carried out with the TZVP basis set and eight Laplace quadrature points. Eight Laplace quadrature points provide a satisfying accuracy of the Laplace error function of $F^{\text{Lap}} < 2.5 \cdot 10^{-8}$ for all glycine chains. In Fig. 4 and 5 the computational time per CC2 iteration is plotted. The results are fitted to polynomial functions of the chain length N_{gly}:

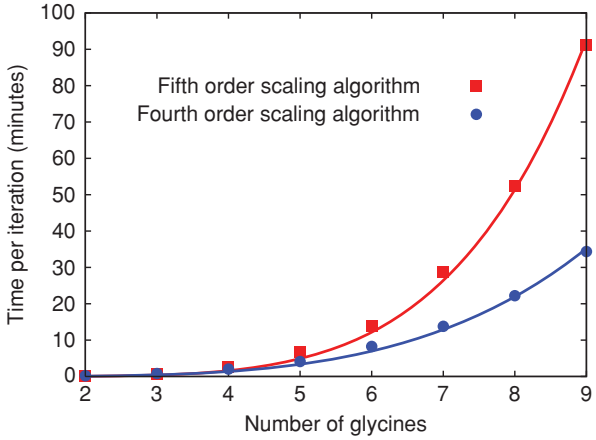


FIG. 4. Timings for CC2 ground state calculation tested at a glycines chain: CPU time per iteration (minutes) versus the number of glycines N_{gly}.

$$f(N_{\text{gly}}) = \alpha N_{\text{gly}}^5, \tag{32}$$

$$g(N_{\text{gly}}) = \beta N_{\text{gly}}^4. \tag{33}$$

For the excited state β is about four times higher than α. The fit of the ground state calculations results in a $\frac{\beta}{\alpha}$ ratio of 3.4. Accordingly for small system sizes the fourth order scaling algorithm is more expensive than the fifth order scaling one. However, the break-even point is already met with a chain of three glycines, where the fourth order scaling algorithm is about as fast as the fifth order scaling one. With computational times of about 50 s for a ground state iteration and about 70 s for an excited state iteration, the computational effort for three glycines is still small. From Figs. 4 and 5 one can see that for systems larger than three glycines the fourth

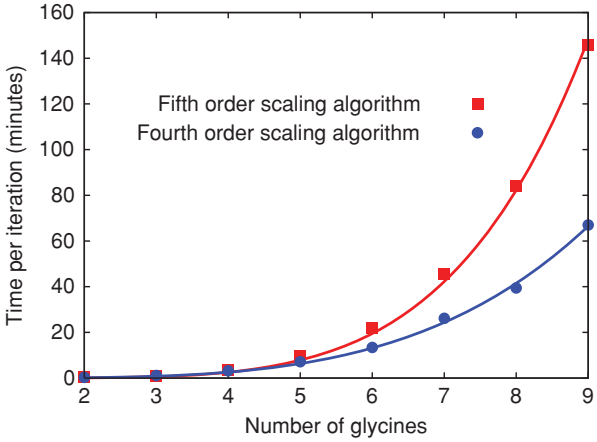


FIG. 5. Timings for CC2 excited state calculation tested at a glycines chain: CPU time per iteration (minutes) versus the number of glycines N_{gly}.

Downloaded 09 May 2011 to 134.147.252.238. Redistribution subject to AIP license or copyright; see http://jcp.aip.org/about/rights_and_permissions

order scaling algorithm is faster and the savings in computational time increase rapidly. For a chain with seven glycines the fifth order scaling algorithm is already about twice as expensive (factor 2.1 for the ground state and 1.7 for the excited state) as the fourth order scaling one.

C. Accuracy of SOS-CC2 and SOS-ADC(2)

To test the accuracy of SOS-CC2 and SOS-ADC(2) in more detail, we benchmarked the vertical excitation energies for a large test set of singlet and triplet states, for which accurate reference data are available from Ref. 31. For better comparison we kept the numbering of the states from Ref. 31, which excludes Rydberg states. All calculations were carried out with the TURBOMOLE program package[13] using the frozen core approximation, where only valence electrons are correlated.

The CC3 reference data from Ref. 31 refer to the aug-cc-pVTZ basis set. In cases where CC3 calculations with the aug-cc-pVTZ basis set could not be achieved, CC3 data calculated with the TZVP basis set were used and combined with basis set corrections from CC2 or CCSDR(3). To correct for the basis set effects, results from calculations with the TZVP and the aug-cc-pVTZ basis set had to be assigned to each other. This has been done in Ref. 32. We repeated the CC2 calculations with the TZVP and aug-cc-pVTZ basis to have a proper reference for assigning the SOS results. Some of the excited states calculated with CC2/aug-cc-pVTZ could not clearly be assigned to the TZVP results. Since it is not clear if the basis set correction for these states is reliable, we excluded them in the present study. We also excluded excited states that contain a strong double excitation character ($\%R_1(\mathrm{CC3}) < 80\%$, see Ref. 33 for comparison). The results for the remaining benchmark set of 89 singlet and 71 triplet excited states can be seen from Tables V and VI.

In the following the error of CC2, SOS-CC2, and SOS-ADC(2) is estimated as

$$\Delta E_{\mathrm{method}} = E_{\mathrm{method}} - E_{\mathrm{CC3}}. \tag{34}$$

The maximum absolute error (MAX), mean error (ME), mean absolute error (MAE), and standard deviation (SD) for unscaled CC2, SOS-CC2, and SOS-ADC(2) are given in Table III. The MAX of all methods is high, as there are still some triplet states in the test set that have sizeable double excitation contributions. This is due to the fact that the $\%R_1$ criterion cannot be applied to triplet states in the same way as to singlet states. For the following triplet states a $\%R_1$ criterion of less than 96% indicates a strong double excitation character: 1 $^3E_{2g}$ in benzene, 3 $^3B_{1g}$ in naphthalene, and 3 $^3A_1$ and 3 $^3B_2$ in pyridine. The 2 ^3A_g state of naphthalene is perturbed by the close by lying 3 ^3A_g state with a $\%R_1$ criterion of 95%. For all other triplet states the CC2 results deviate by less than 0.3 eV from the CC3 reference values. The 1 $^1B_2$ state of pyrrole is the only singlet state, where CC2 has a deviation from the CC3 values of more than 0.3 eV. For this state, the basis set extrapolation done by CCSDR(3) (Ref. 32) results in a change of the CC3 value of 0.51 eV from the TZVP basis to aug-cc-pVTZ. As the CC2 and CC3 results obtained in the TZVP basis set[33] agree well, it might be that the basis set correction applied to the CC3 value is not reliable in this case. SOS-CC2 and SOS-ADC(2) provide errors of more than 0.3 eV only for the above discussed states, where unscaled CC2 also fails.

TABLE III. Maximum absolute error (MAX), mean error (ME), mean absolute error (MAE), and standard deviation (SD) in eV for the test set from Tables V and VI.

	CC2	SOS-CC2	SOS-ADC(2)
MAX	0.65	0.67	0.69
ME	0.09	0.22	0.20
MAE	0.12	0.24	0.22
SD	0.14	0.16	0.18

The mean error and mean absolute error of SOS-CC2 and SOS-ADC(2) are about twice as high as for unscaled CC2. This is due to the fact that the spin scaled methods are more blue shifted. The differences between SOS-CC2 and SOS-ADC(2) are small. The standard deviation of SOS-CC2 of 0.16 eV is only slightly higher than for unscaled CC2. This means that the error distribution of CC2 is not affected strongly by the spin scaling. SOS-ADC(2) provides a standard deviation of 0.18 eV, which is slightly higher than for SOS-CC2. All together we conclude that SOS-CC2 and SOS-ADC(2) predict excitation energies with an accuracy comparable to that of unscaled CC2.

D. Applications

In this section two applications are presented. The first one comprises two organic dyes, which are candidates to be used as sensitizers in organic solar cells: 3-(5-(4-(diphenylamino)styryl)thiophen-2-yl)-2-cyanoacrylic acid (D5) and 5-(4-(bis(4-methoxyphenylamino)-styryl)thiophen-2-yl)-2-cyanoacrylic acid (D9). The structures of the two molecules are depicted in Figs. 6 and 7. These dyes were already investigated with SOS-CIS(D)[34] and compared to experimental data in solution from Ref. 35. We used structures optimized with B3LYP and the 6-31G(d) basis set including the SM8 solvent model[36] from Ref. 34 and calculated vertical excitation energies with unscaled CC2 and Laplace-transformed SOS-CC2 using the aug-cc-pVTZ basis set. For D5 the SOS-CC2 value of 2.85 eV deviates less from the experimental value of 2.81 eV than the result obtained with unscaled CC2 (2.50 eV). We get the same picture for D9, where SOS-CC2 provides an excitation energy of 2.74 eV and unscaled CC2 of 2.37 eV, which has to be compared to an experimental value of 2.68 eV. However, one has to take into account that the ground state structures account for solvent effects, but no solvent model is included in the calculation of the vertical excitation energies.

The computational times for the conventional algorithm for parallel calculations of one excited state on eight processors are 95 h for D5 and 257 h for D9, respectively. The Laplace-transformed SOS-CC2 algorithm requires computational times of 58 h for D5 and 114 h for D9 under the same conditions. For the Laplace-transformed algorithm 11 grid points are used for the numerical quadrature procedure, which

Downloaded 09 May 2011 to 134.147.252.238. Redistribution subject to AIP license or copyright; see http://jcp.aip.org/about/rights_and_permissions

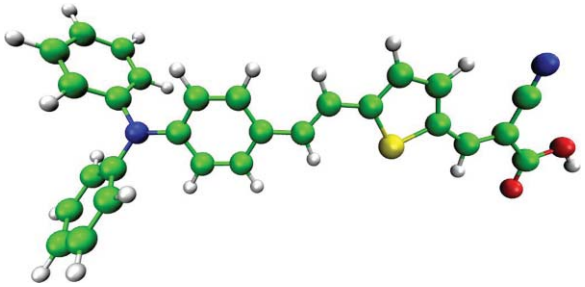


FIG. 6. Structure of the dye D5.

provides a value of the Laplace error function of less than 10^{-12}. Although a highly accurate grid is used for the Laplace integration, the fourth order scaling algorithm provides significant savings in computational time. For D5 (53 atoms) the ratio between the fifth and fourth order scaling algorithm is 1.6 and for D9 (61 atoms) already 2.3. This example shows how the savings in computational time increase with increasing system size for parallel calculations.

Finally we applied the Laplace-transformed SOS-CC2 method to the calculation of vertical excitation energies of a chlorophyll molecule. This system has 137 atoms and, using the TZVP basis set, 176 occupied and 1421 virtual orbitals and 4455 auxiliary basis functions for the RI approximation. The ground state structure was optimized with B3LYP/TZVP and is shown in Fig. 8. For this system size excited state calculations for several roots are hardly feasible any more with the conventional CC2 algorithm. The results of the SOS-CC2 calculation are given in Table IV . For comparison, also experimental values measured in an ether solution[37] and computed vertical excitation energies obtained with BP/SV(P) (Ref. 38) are listed. The two lowest electronic transition of the chlorophyll molecule are split in the experimental spectrum due to vibronic coupling.[38] SOS-CC2 reproduces correctly two low lying electronic transitions in this energy region, whereas DFT with BP/SV(P) provides four electronic states with an excitation energy up to 2.32 eV. These unphysical transitions are due to artificial charge transfer states that occur in DFT calculations using semilocal functionals. The first and second excitations are reproduced well with the SOS-CC2 method with deviations of 0.1 eV or less from the experimental value.

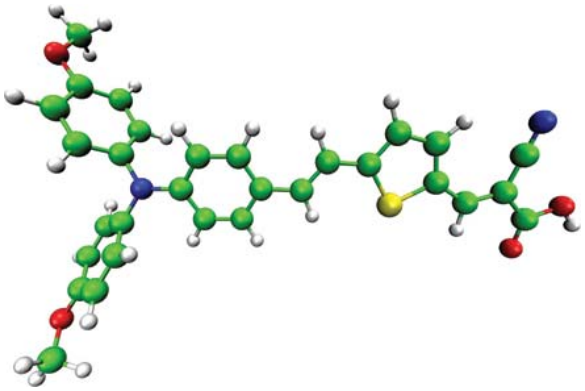


FIG. 7. Structure of the dye D9.

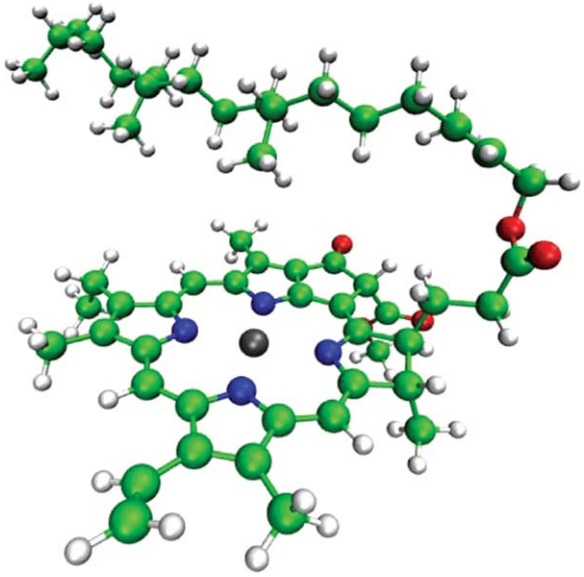


FIG. 8. Structure of the chlorophyll molecule.

The third electronic transition is blue shifted by 0.51 eV with SOS-CC2, which is probably due to solvent effects.

The SOS-CC2 calculation was carried out using 14 grid points for the Laplace transformation, which corresponds to a value of the Laplace error function of $2.5 \cdot 10^{-15}$. The wall time for the time-determining steps per excited state per iteration was 3 h on seven processors. We estimated that the time-determining steps of the conventional CC2 algorithm would have taken 7.5 h per excited state iteration under the same conditions. By using only seven Laplace grid points for the SOS-CC2 calculation, which still provides a satisfying value of the Laplace error function of $1.3 \cdot 10^{-7}$, one could reduce the computational costs of the time-determining steps of SOS-CC2 to only 1.5 h per iteration. Thus the Laplace-transformed SOS-CC2 algorithm results in a speed-up of a factor of five for this system size.

Additional savings can be obtained by using smaller grids for the numerical integration during the iterative solution of the ground state cluster equations or the non-linear eigenvalue problem. The largest grid that fulfills the criteria for F^{Lap} is only needed for the final iterations. For excited state calculations, where several iterations are done with the same grid or several eigenvectors are determined simultaneously, the

TABLE IV. Vertical excitations energies (eV) of the chlorophyll molecule calculated with SOS-CC2 (aug-cc-pVTZ) and DFT (BP, SV(P)) (Ref. 38) compared to experimental values measured in ether (Ref. 37).

Exp.	SOS-CC2	DFT
1.88/2.02[a]	2.09	2.00
		2.04
2.16/2.34[a]	2.44	2.18
		2.32
		⋮
2.90	3.41	2.75

[a]Split due to vibronic coupling.

Downloaded 09 May 2011 to 134.147.252.238. Redistribution subject to AIP license or copyright; see http://jcp.aip.org/about/rights_and_permissions

TABLE V. Vertical excitation energies for singlet states in eV calculated with CC2, SOS-CC2 and SOS-ADC(2), and the aug-cc-pVTZ basis set. CC3 results from Ref. 31 are given for comparison.

Molecule	State	CC3	CC2	SOS-CC2	SOS-ADC(2)
Ethene	1^1B_{1u}	7.89	7.90	7.99	7.96
E-Butadiene	1^1B_u	6.21	6.13	6.32	6.28
E-Hexatriene	1^1B_u	5.32	5.18	5.42	5.37
E-Octatetraene	1^1B_u	4.84	4.53	4.81	4.75
Cyclopropene	1^1B_1	6.67	6.73	6.92	6.94
	1^1B_2	6.68	6.72	6.95	6.92
Cyclopentadiene	1^1B_2	5.49	5.47	5.63	5.59
	3^1A_1	8.14	8.19	8.35	8.36
Norbornadiene	1^1A_2	5.37	5.30	5.67	5.66
	1^1B_2	6.21	6.09	6.63	6.64
	2^1B_2	7.49	7.50	7.87	7.90
	2^1A_2	7.22	7.17	7.63	7.66
Benzene	1^1B_{2u}	5.03	5.22	4.98	4.99
	1^1B_{1u}	6.42	6.45	6.31	6.29
	1^1E_{1u}	7.14	7.12	7.25	7.26
Naphthalene	1^1B_{3u}	4.25	4.38	4.27	4.28
	1^1B_{2u}	4.82	4.75	4.89	4.86
	2^1A_g	5.90	6.07	5.96	5.98
	2^1B_{3u}	6.11	6.02	6.21	6.20
	2^1B_{2u}	6.36	6.35	6.43	6.43
	2^1B_{1g}	6.46	6.44	6.58	6.59
Furan	1^1B_2	6.26	6.37	6.44	6.45
	2^1A_1	6.51	6.70	6.74	6.74
	3^1A_1	8.13	8.23	8.35	8.35
Pyrrole	2^1A_1	6.27	6.42	6.34	6.35
	1^1B_2	6.20	6.85	6.87	6.89
	3^1A_1	7.60	7.81	7.92	7.95
Imidazole	$2^1A'$	6.25	6.40	6.45	6.46
	$1^1A''$	6.65	6.69	6.90	6.88
	$3^1A'$	6.73	6.91	6.87	6.87
	$2^1A''$	7.57	7.64	8.02	8.03
	$4^1A'$	8.51	8.68	8.82	8.84
Pyridine	1^1B_2	5.12	5.26	5.03	5.04
	1^1B_1	4.95	4.97	5.29	5.29
	1^1A_2	5.41	5.27	5.65	5.64
	2^1A_1	6.60	6.64	6.53	6.49
	2^1B_2	7.33	7.32	7.43	7.43
	3^1A_1	7.39	7.43	7.52	7.54
Pyrazine	1^1B_{3u}	4.13	4.12	4.42	4.45
	1^1A_u	4.98	4.86	5.29	5.32
	1^1B_{2u}	4.97	5.07	4.85	4.88
	1^1B_{2g}	5.65	5.79	6.03	6.04
	1^1B_{1g}	6.69	6.61	7.04	7.06
	1^1B_{1u}	6.83	6.86	6.76	6.73
	2^1B_{2u}	7.81	7.82	7.88	7.90
Pyrimidine	1^1B_1	4.43	4.37	4.72	4.70
	1^1A_2	4.85	4.75	5.08	5.05
	1^1B_2	5.34	5.46	5.23	5.22
	2^1A_1	6.82	6.94	6.82	6.76
	3^1A_1	7.53	7.53	7.68	7.66
	2^1B_2	7.82	7.82	7.94	7.89
Pyridazine	1^1B_1	3.85	3.79	4.13	4.15
	1^1A_2	4.44	4.30	4.74	4.76
	2^1A_1	5.20	5.32	5.08	5.09
	2^1A_2	5.66	5.70	6.05	6.07
	1^1B_2	6.68	6.79	6.64	6.63
	2^1B_1	6.33	6.27	6.67	6.69
	2^1B_2	7.33	7.33	7.47	7.48
s-Triazine	$1^1A_1''$	4.70	4.60	4.87	4.82
	$1^1A_2''$	4.71	4.71	5.11	5.09
	$1^1E''$	4.75	4.68	5.03	4.99
	$1^1A_2'$	5.71	5.80	5.56	5.53
	$2^1A_1'$	7.18	7.26	7.24	7.14
	$1^1E'$	7.84	7.88	7.99	7.89
	$2^1E''$	7.78	7.97	8.18	8.14
s-Tetrazine	1^1B_{3u}	2.46	2.39	2.73	2.77
	1^1A_u	3.78	3.61	4.10	4.15
	1^1B_{1g}	4.87	5.00	5.27	5.29
	1^1B_{2u}	5.08	5.16	4.90	4.91
	1^1B_{2g}	5.28	5.45	5.75	5.78
	2^1A_u	5.39	5.40	5.75	5.78
	2^1B_{1g}	6.80	6.82	7.24	7.28
	2^1B_{3u}	6.60	6.61	7.03	7.07
	2^1B_{2u}	8.33	8.45	8.57	8.55
	2^1B_{3g}	8.51	8.85	8.76	8.83
Formaldehyde	1^1A_2	3.88	4.00	4.15	4.00
	1^1B_1	9.05	9.19	9.32	9.17
	2^1A_1	9.31	9.50	9.67	9.45
Acetone	1^1A_2	4.38	4.45	4.58	4.41
	1^1B_1	9.04	9.11	9.30	9.15
p-Benzoquinone	1^1B_{1g}	2.74	2.76	3.24	3.12
	1^1A_u	2.86	2.88	3.35	3.20
	1^1B_{3g}	4.44	4.53	4.93	4.98
	1^1B_{1u}	5.47	5.46	5.84	5.69
	2^1B_{3g}	7.16	7.17	7.57	7.49
Formamide	$1^1A''$	5.55	5.59	5.71	5.50
	$2^1A'$	7.35	7.46	7.62	7.50
Acetamide	$1^1A''$	5.62	5.61	5.75	5.54
Propanamide	$1^1A''$	5.65	5.62	5.77	5.56

intermediate N_z^{QP} (see Eq. (22)) needs to be evaluated only once, which reduces the costs for the Laplace part by additional 25%.

V. SUMMARY

We presented a fourth order scaling algorithm for Laplace-transformed SOS-CC2 and SOS-ADC(2) energies of ground and excited states. Using a test set with 89 singlet and 71 triplet excitations we showed that for vertical electronic excitations SOS-CC2 provides an accuracy comparable to that of unscaled CC2. We developed a criterion for the numerical error of the approximated Laplace transformation and demonstrated its reliability in the case of ground and excited states. For usual applications seven to eight grid points for the numerical Laplace transformation seem to be sufficient. The fourth order scaling algorithm provides computational savings for systems larger than 20 to 30 atoms. From that point on the speed-up increases rapidly. For system sizes of 50 to 60 atoms the fourth order scaling algorithm is about twice as fast a the conventional one. We also presented an application to a chlorophyll molecule with 137 atoms that is hardly feasible any more with the conventional CC2 algorithm. For this system size the fourth order scaling algorithm provides a speed-up of a factor of five.

Downloaded 09 May 2011 to 134.147.252.238. Redistribution subject to AIP license or copyright; see http://jcp.aip.org/about/rights_and_permissions

TABLE VI. Vertical excitation energies for triplet states in eV calculated with CC2, SOS-CC2 and SOS-ADC(2), and the aug-cc-pVTZ basis set. CC3 results from Ref. 31 are given for comparison.

Molecule	State	CC3	CC2	SOS-CC2	SOS-ADC(2)
Ethene	1^3B_{1u}	4.50	4.56	4.55	4.56
E-Butadiene	1^3B_u	3.34	3.43	3.51	3.51
	1^3A_g	5.15	5.25	5.18	5.18
E-Hexatriene	1^3B_u	2.71	2.80	2.94	2.94
	1^3A_g	4.33	4.42	4.39	4.38
E-Octatetraene	1^3B_u	2.32	2.42	2.60	2.60
	1^3A_g	3.69	3.78	3.79	3.78
Cyclopropene	1^3B_2	4.28	4.40	4.43	4.43
	1^3B_1	6.40	6.44	6.69	6.71
Cyclopentadiene	1^3B_2	3.26	3.37	3.41	3.41
	1^3A_1	5.09	5.22	5.07	5.07
Norbornadiene	1^3A_2	3.68	3.72	3.85	3.85
	1^3B_2	4.16	4.25	4.19	4.19
Benzene	1^3B_{1u}	4.12	4.33	4.28	4.29
	1^3E_{1u}	4.81	5.05	4.96	4.96
	1^3B_{2u}	5.78	5.86	5.95	5.93
	1^3E_{2g}	7.45	7.92	7.84	7.84
Naphthalene	1^3B_{2u}	3.09	3.25	3.30	3.29
	1^3B_{3u}	4.09	4.28	4.26	4.25
	1^3B_{1g}	4.42	4.59	4.56	4.55
	2^3B_{2u}	4.56	4.81	4.74	4.73
	2^3B_{3u}	4.92	4.93	5.09	5.06
	1^3A_g	5.42	5.67	5.53	5.52
	2^3B_{1g}	6.12	6.07	6.39	6.40
	2^3A_g	6.17	6.53	6.64	6.65
	3^3A_g	6.65	6.80	6.94	6.93
	3^3B_{1g}	6.67	7.14	7.18	7.18
Furan	1^3B_2	4.11	4.33	4.30	4.29
	1^3A_1	5.43	5.61	5.43	5.40
Pyrrole	1^3B_2	4.44	4.64	4.59	4.59
	1^3A_1	5.42	5.63	5.49	5.47
Imidazole	$1^3A'$	4.65	4.85	4.82	4.80
	$2^3A'$	5.64	5.86	5.75	5.74
	$1^3A''$	6.25	6.32	6.53	6.50
	$3^3A'$	6.38	6.57	6.63	6.63
	$4^3A'$	7.25	7.51	7.61	7.63
	$2^3A''$	7.29	7.30	7.73	7.75
Pyridine	1^3A_1	4.28	4.48	4.44	4.44
	1^3B_1	4.42	4.46	4.80	4.80
	1^3B_2	4.72	4.93	4.89	4.88
	2^3A_1	4.96	5.24	5.12	5.11
	1^3A_2	5.35	5.23	5.65	5.65
	2^3B_2	6.22	6.34	6.42	6.38
	3^3A_1	7.59	8.11	8.00	8.00
	3^3B_2	7.29	7.85	7.90	7.95
s-Tetrazine	1^3B_{3u}	1.87	1.83	2.19	2.23
	1^3A_u	3.49	3.39	3.89	3.94
	1^3B_{1g}	4.18	4.27	4.52	4.52
	1^3B_{1u}	4.36	4.66	4.48	4.49
	1^3B_{2u}	4.39	4.65	4.53	4.52
	1^3B_{2g}	4.89	4.99	5.32	5.33
	2^3A_u	4.96	4.98	5.39	5.41
	2^3B_{1u}	5.32	5.59	5.52	5.49
	2^3B_{2g}	5.97	5.98	6.52	6.56
	2^3B_{1g}	6.54	6.65	7.10	7.15
	2^3B_{3u}	6.45	6.43	6.89	6.92
	2^3B_{2u}	7.21	7.52	7.62	7.68
Formaldehyde	1^3A_2	3.49	3.52	3.77	3.64
	1^3A_1	5.86	6.12	5.99	5.91
Acetone	1^3A_2	4.05	4.07	4.28	4.13
	1^3A_1	6.07	6.31	6.24	6.14
p-Benzoquinone	1^3B_{1g}	2.50	2.46	2.98	2.87
	1^3A_u	2.61	2.58	3.10	2.96
	1^3B_{1u}	3.02	3.18	3.27	3.24
	1^3B_{3g}	3.37	3.46	3.65	3.66
Formamide	$1^3A''$	5.28	5.27	5.48	5.29
	$1^3A'$	5.69	5.88	5.93	5.85
Acetamide	$1^3A''$	5.35	5.33	5.55	5.36
	$1^3A'$	5.71	6.02	6.09	6.00
Propanamide	$1^3A''$	5.38	5.35	5.57	5.38
	$1^3A'$	6.08	6.02	6.11	6.02

The SOS version of the algebraic diagrammatic construction scheme through second order, ADC(2), shows only small deviations from the SOS-CC2 values. SOS-ADC(2) will thus be a cost-efficient alternative for geometry optimizations, since for the evaluation of excited state gradients with ADC(2) fewer equations need to be solved than for CC2. Work in this direction is in progress and will be reported in a forthcoming publication.

[1] S. Grimme, J. Chem. Phys. **118**, 9095 (2003).
[2] Y. Jung, R. C. Lochan, A. D. Dutoi, and M. Head-Gordon, J. Chem. Phys. **121**, 9793 (2004).
[3] S. Grimme and E. I. Izgorodina, Chem. Phys. **305**, 223 (2004).
[4] Y. M. Rhee and M. Head-Gordon, J. Phys. Chem. **111**, 5314 (2007).
[5] Y. M. Rhee, D. Casanova, and M. Head-Gordon, J. Chem. Theory Comput. **5**, 1224 (2009).
[6] O. Christiansen, H. Koch, and P. Jørgensen, Chem. Phys. Lett. **243**, 409 (1995).
[7] C. Hättig and F. Weigend, J. Chem. Phys. **113**, 5154 (2000).
[8] A. Köhn and C. Hättig, J. Chem. Phys. **119**, 5021 (2003).
[9] C. Hättig and A. Köhn, J. Chem. Phys. **117**, 6939 (2002).
[10] C. Hättig, O. Christiansen, and P. Jørgensen, J. Chem. Phys. **108**, 8331 (1998).
[11] D. Kats, T. Korona, and M. Schütz, J. Chem. Phys. **125**, 104106 (2006).
[12] A. Hellweg, S. A. Grün, and C. Hättig, Phys. Chem. Chem. Phys. **10**, 1 (2008).
[13] TURBOMOLE (V6.2).
[14] M. Head-Gordon, M. Oumi, and D. Maurice, Mol. Phys. **96**, 593 (1999).
[15] J. Schirmer, Phys. Rev. A **26**, 2395 (1982).
[16] A. K. Wilson and J. Almlöf, Theor. Chim. Acta **95**, 49 (1997).
[17] D. Kats, D. U. Usvyat, S. Loibl, T. Merz, and M. Schütz, J. Chem. Phys. **130**, 127101 (2009).
[18] A. Schäfer, H. Horn, and R. Ahlrichs, J. Chem. Phys. **97**, 2571 (1992).
[19] A. Schäfer, C. Huber, and R. Ahlrichs, J. Chem. Phys. **100**, 5829 (1994).
[20] F. Weigend, M. Häser, H. Patzelt, and R. Ahlrichs, Chem. Phys. Lett. **294**, 143 (1998).
[21] F. Weigend, F. Furche, and R. Ahlrichs, J. Chem. Phys. **119**, 12753 (2003).
[22] C. Hättig, Phys. Chem. Chem. Phys. **7**, 59 (2005).
[23] T. H. Dunning, J. Chem. Phys. **90**, 1007 (1989).
[24] R. A. Kendall, T. H. Dunning, and R. J. Harrison, J. Chem. Phys. **96**, 6796 (1992).
[25] D. E. Woon and T. H. Dunning, J. Chem. Phys. **98**, 1358 (1993).
[26] K. A. Peterson and C. Puzzarini, Theor. Chim. Acta **114**, 283 (2005).
[27] D. Figgen, G. Rauhut, M. Dolg, and H. Stoll, Chem. Phys. **311**, 227 (2005).
[28] F. Weigend, A. Köhn, and C. Hättig, J. Chem. Phys. **116**, 3175 (2002).
[29] All basis set are taken from the basis set library of TURBOMOLE V6.2.
[30] K. A. Peterson and T. H. Dunning, J. Chem. Phys. **117**, 10548 (2002).
[31] M. R. Silva-Junior, M. Schreiber, S. P. A. Sauer, and W. Thiel, J. Chem. Phys. **133**, 174318 (2010).

Downloaded 09 May 2011 to 134.147.252.238. Redistribution subject to AIP license or copyright; see http://jcp.aip.org/about/rights_and_permissions

[32]M. R. Silva-Junior, S. P. A. Sauer, M. Schreiber, and W. Thiel, Mol. Phys. **108**, 453 (2010b).
[33]M. Schreiber, M. R. Silva-Junior, S. P. A. Sauer, and W. Thiel, J. Chem. Phys. **128**, 134110 (2008).
[34]D. Casanova, F. P. Rotzinger, and M. Grätzel, J. Chem. Theory Comput. **6**, 1219 (2010).
[35]D. P. Hagberg, J.-H. Yum, H. Lee, F. D. Angelis, T. Marinado, K. M. Karlsson, R. Humphry-Baker, L. Sun, A. Hagfeldt, M. Grätzel, and M. K. Nazeeruddin, J. Am. Chem. Soc. **130**, 6259 (2008).
[36]D. Casanova, private communication (2010).
[37]C. Houssier and K. Sauer, J. Am. Chem. Soc. **92**, 779 (1970).
[38]D. Sundholm, Chem. Phys. Lett. **302**, 480 (1999).

Downloaded 09 May 2011 to 134.147.252.238. Redistribution subject to AIP license or copyright; see http://jcp.aip.org/about/rights_and_permissions